Design study of highly sensitive nanowire-enhanced surface plasmon resonance biosensors using rigorous coupled wave analysis

Kyung Min Byun and Sung June Kim

School of Electrical Engineering, Seoul National University, Seoul, Korea 151-742

Donghyun Kim

School of Electrical and Electronic Engineering, Yonsei University, Seoul, Korea 120-749
kimd@yonsei.ac.kr

Abstract: In this study, we investigated the sensitivity enhancement in nanowire-based surface plasmon resonance (SPR) biosensors using rigorous coupled wave analysis (RCWA). The enhancement, enabled by the excitation of localized surface plasmons in gold nanowires, offers improved performance in sensitivity as well as in reproducibility and customizability. Calculation results found that a T-profile provides higher sensitivity than an inverse T-profile in general and also determined optimum design parameters. Our study on a nanowire-enhanced SPR biosensor demonstrates the potential for significant improvement in the sensitivity through the nanowire-mediated localized SPR.

OCIS codes: (050.2770) Gratings; (130.6010) Sensors; (240.6680) Surface plasmons

References

1. B. Rothenhäusler and W. Knoll, "Surface-plasmon microscopy," Nature **332**, 615-617 (1988).
2. K. Matsubara, S. Kawata, and S. Minami, "Optical chemical sensor based on surface plasmon measurement," Appl. Opt. **27**, 1160-1163 (1988).
3. C. Nylanderm B. Liedberg, and T. Lind, "Gas detection by means of surface plasmon resonance," Sens. Actuators **3**, 79-88 (1982-1983).
4. D. Hall, "Use of optical biosensors for the study of mechanically concerted surface adsorption processes," Anal. Biochem. **288**, 109-125 (2001).
5. L. S. Jung, C. T. Campbell, T. M. Chinowsky, M. N. Mar, and S. S. Yee, "Quantitative interpretation of the response of surface plasmon resonance sensors to adsorbed films," Langmuir **14**, 5636-5648 (1998).
6. D. R. Baselt, G. U. Lee, K. M. Hansen, L. A. Chrisey, and R. J. Colton, "A high-sensitivity micromachined biosensor," Proceedings of the IEEE **85**, 672-680 (1997).
7. L. He, M. D. Musick, S. R. Nicewarner, F. G. Salinas, S. J. Benkovic, M. J. Natan, and C. D. Keating, "Colloidal Au-enhanced surface plasmon resonance for ultrasensitive detection of DNA hybridization," J. Am. Chem. Soc. **122**, 9071-9077 (2000).
8. M. D. Malinsky, K. L. Kelly, G. C. Schatz, and R. P. Van Duyne, "Chain length dependence and sensing capabilities of the localized surface plasmon resonance of silver nanoparticles chemically modified with alkanethiol self-assembled monolayers," J. Am. Chem. Soc. **123**, 1471-1482 (2001).
9. A. J. Haes and R. P. Van Duyne, "A nanoscale optical biosensor: sensitivity and selectivity of an approach based on the localized surface plasmon resonance spectroscopy of triangular silver nanoparticles," J. Am. Chem. Soc. **124**, 10596-10604 (2002).
10. M. G. Moharam and T. K. Gaylord, "Diffraction analysis of dielectric surface-relief gratings," J. Opt. Soc. Am. **72**, 1385-1392 (1982).
11. M. G. Moharam and T. K. Gaylord, "Rigorous coupled-wave analysis of metallic surface-relief gratings," J. Opt. Soc. Am. A **3**, 1780-1787 (1986).
12. Y. Kanamori, K. Hane, H. Sai, and H. Yugami, "100 nm period silicon antireflection structures fabricated using a porous alumina membrane mask," Appl. Phys. **78**, 142-143 (2001).
13. T. R. Jensen, L. Kelley, A. Lazarides, and G. C. Schatz, "Electrodynamics of noble metal nanoparticles and nanoparticle clusters," J. Cluster Sci. **10**, 295-317 (1999).
14. S. Park, G. Lee, S. H. Song, C. H. Oh, and P. S. Kim, "Resonant coupling of surface plasmons to radiation modes by use of dielectric gratings," Opt. Lett. **28**, 1870-1872 (2003).

#7078 - $15.00 US Received 6 April 2005; revised 27 April 2005; accepted 4 May 2005

15. J. Lermé, "Introduction of quantum finite-size effects in the Mie's theory for a multilayered metal sphere in the dipolar approximation: application to free and matrix-embedded noble metal clusters," Eur. Phys. J. D **10**, 265-277 (2000).
16. E. Moreno, D. Erni, C. Hafner, and R. Vahldieck, "Multiple multipole method with automatic multipole setting applied to the simulation of surface plasmons in metallic nanostructures," J. Am. Opt. Soc. A **19**, 101-111 (2002).
17. K. M. Byun, D. Kim, and S. J. Kim, "Investigation of the sensitivity enhancement of nanoparticle-based surface plasmon resonance biosensors using rigorous coupled-wave analysis," in Plasmonics in Biology and Medicine II, T. Vo-Dinh, J. R. Lakowicz, and Z. K. Gryczynski, eds., Proc SPIE **5703**, 61-70 (2005).
18. E. Hutter, S. Cha, J-F. Liu, J. Park, J. Yi, J. H. Fendler, and D. Roy, "Role of substrate metal in gold nanoparticle enhanced surface plasmon resonance imaging," J. Phys. Chem. B **105**, 8-12 (2001).
19. L. A. Lyon, M. D. Musick, and M. J. Natan, "Colloidal Au-enhanced surface plasmon resonance immunosensing," Anal. Chem. **70**, 5177-5183 (1998).
20. L. A. Lyon, D. J. Pena, and M. J. Natan, "Surface plasmon resonance of Au colloid-modified Au films: Particle size dependence," J. Phys. Chem. B **103**, 5826-5831 (1999).
21. E. D. Palik, *Handbook of Optical Constants of Solids*, Academic Press, Orlando, FL (1985).
22. G. Schider, J. R. Krenn, W. Gotschy, B. Lamprecht, H. Ditlbacher, A. Leitner, and F. R. Aussenegg, "Optical properties of Ag and Au nanowire gratings," J. Appl. Phys. **90**, 3825-3830 (2001).
23. W. Gotschy, K. Vonmetz, A. Leitner, and F. R. Aussenegg, "Optical dichroism of lithographically designed silver nanoparticle films," Opt. Lett. **21**, 1099-1101 (1996).
24. J. P. Kottmann and O. J. F. Martin, "Retardation-induced plasmon resonances in coupled nanoparticles," Opt. Lett. **26**, 1096-1098 (2001).

1. Introduction

Surface plasmon resonance (SPR) has been widely used in a variety of sensing applications, since it provides rapid, label-free and array-based real-time sensing capability of detecting biochemical reactions on a surface.[1,2,3] The highest sensitivity that was reported of an SPR biosensor based on a traditional configuration is approximately 1 pg/mm^2, corresponding to a change of 5 x 10^{-7} in refractive index.[4,5] While other sensing mechanisms, such as cantilever based ones using an atomic force tip to mount antibodies for specificity which result in different resonance vibrations with binding, are known to offer comparable sensitivity,[6] an SPR based biosensor is extremely simple in structure and has been commercially available as an economic solution to many sensing needs. However, it suffers from insufficient sensitivity for some applications, for example, the sensing of aerosol or gas-phase release of toxins. In order to overcome the sensitivity limitation, nanoparticle-based SPR biosensors have drawn tremendous interests in recent years, since it has been empirically shown that applying nanoparticles may significantly enhance its sensitivity by 1-2 orders of magnitude.[7,8,9] In a conventional SPR biosensor using an attenuated total reflection scheme, the performance of the sensor is determined by the surface plasmon polaritons (SPPs) excited on a thin metal film and propagating along the surface. However, the use of noble metal nanostructures allows strong optical coupling of incident light to resonances, so called localized surface plasmons (LSPs), which are collective electron oscillations localized in the metallic nanostructure. Various interactions between LSPs, SPPs, and binding biomaterial in the presence of nanostructures can lead to different resonance properties with an additional shift of resonance angle, as well as changes in the reflectance amplitude and resonance width, resulting in enhanced sensitivity of a SPR biosensor.

Based on the importance of the LSP-SPP interactions in the sensitivity enhancement of a SPR biosensor, this feasibility study intends to investigate the electromagnetic coupling of SPPs that are nearly localized, whereby the sensitivity enhancement of nanowire-based SPR biosensors are theoretically investigated. For this goal, we study a model that employs nanowires using well-established rigorous coupled wave analysis (RCWA).[10,11] The use of nanowires on a gold thin film results in a structure that can provide reproducible performance. Also, the design of nanowires can be customized when it is desired to meet specific sensitivity requirement in practical applications. We are particularly interested in the impact of geometrical parameters such as nanowire period and its profile and size on the coupling of LSPs in nanowires and thus the sensitivity enhancement in a nanowire-based SPR biosensor.

#7078 - $15.00 US Received 6 April 2005; revised 27 April 2005; accepted 4 May 2005

2. Numerical method

When the size of nanostructure is smaller than 100 nm, the calculation becomes difficult and the convergence problem is not easy to solve due to extremely rapid variations of the field that occur on very short distances. RCWA, however, has been successfully applied for numerical calculations to explain experimental results of nanostructures.[12,13,14] The applicability of such a classical approach to a metallic structure on a nanometer scale in size has been the topic of previous studies.[15,16] Their results indicate that experimental observation is in good agreement with classical prediction for size ranges much greater than Fermi wavelength of the conduction electron gas. Convergence in RCWA can be achieved by including a sufficient number of space harmonics. Note that our RCWA routine was found to corroborate experimental results of earlier nanoparticle-based SPR studies by modeling with nanowires.[17]

A schematic diagram of a nanowire-based SPR biosensor model is shown in Fig. 1, where nanowires are represented as a one-dimensional array of gold wires oriented along the y-axis. The gold nanowires are assumed to sit on top of a thin film of a 40 nm thick gold layer, where SPPs are excited, and an attachment layer of chromium with 2 nm thickness. The antibody-analyte binding is modeled with a 1 nm thick self-assembled monolayer (SAM) that is supported by gold nanowires and the thin gold film. Based on the reports that nanostructures of the size ranging from 20 nm to 50 nm produce the strongest and sharpest SPR enhancement,[18,19,20] the nanowires were sized in this range. The complex indices of refraction of the BK7 glass prism substrate and layers of chromium and gold were taken from Ref. 21, determined respectively as 1.5151, 3.48 + 4.36*i*, and 0.18 + 3.0*i* at λ = 633 nm. In our study, we assumed 1,6-hexanedithiol (HDT) for the dielectric SAM and used n(HDT) = 1.526 for layer 4 and 5, which was empirically obtained in Ref. 18. The SAM is extremely thin compared with the wavelength, so that the layer is essentially a lossless dielectric, and its extinction coefficient was thus ignored. The model in Fig. 1 assumes an illumination with a TM-polarized monochromatic plane wave at a fixed wavelength λ = 633 nm as the incidence angle θ is scanned with an angular resolution of 0.01°.

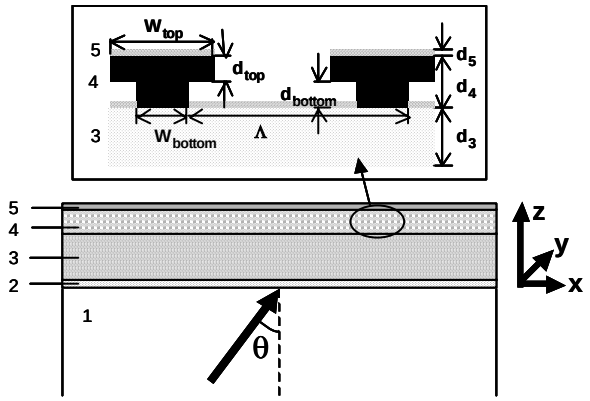

Fig. 1. Schematic diagram of a nanowire-enhanced SPR biosensor with a multilayer model used in this study. A beam is in the *xz*-plane incident at an angle θ. Layer 1, 2, 3, 4, and 5 represent a BK7 glass prism, an attachment film of chromium, gold film supporting SPPs, one-dimensional gold nanowires, and a self-assembled monolayer (SAM), respectively. Dimensions of gold nanowires shown in the inset are decided by a geometry factor (GF). Also, d_3, d_4, and d_5 denote the thickness of gold film, gold nanowires, and a SAM.

In order to investigate the impact of nanowire geometries that affect the sensitivity enhancement, different profiles of gold nanowires were selected for the analysis using parameters shown in the inset of Fig. 1, where w_{top} and w_{bottom} denoting the width of the nanowire top and bottom are either 20 nm or 40 nm. Nanowire depth d_4 ($d_4 = d_{top} + d_{bottom}$) is fixed at 20 nm. Ease of fabrication was also considered in selecting profiles. For convenience, a geometry factor (GF) of nanowires is introduced as d_{top}/d_4 if w_{top} = 40 nm > w_{bottom} = 20 nm

#7078 - $15.00 US Received 6 April 2005; revised 27 April 2005; accepted 4 May 2005

(T-profile), and d_{bottom}/d_4 if w_{top} = 20 nm < w_{bottom} = 40 nm (inverse T-profile). A GF is defined to be equal to 0 if $w_{top} = w_{bottom}$ = 20 nm, and 1 if $w_{top} = w_{bottom}$ = 40 nm. Consequently, T- and inverse T-profiles have an equal volume of nanowires if the GF is the same.

3. Results and discussion

As a quantitative measure of the sensitivity improvement, we introduce a sensitivity enhancement factor (SEF) that represents the impact of nanowires on the SPR sensitivity in reference to a conventional SPR biosensor without nanostructures as

$$SEF = \left| \frac{\Delta\theta_{NWSPR}}{\Delta\theta_{SPR}} \right| = \left| \frac{\theta_{NWSPR}(\text{target analyte}) - \theta_{NWSPR}(\text{no analyte})}{\theta_{SPR}(\text{target analyte}) - \theta_{SPR}(\text{no analyte})} \right|, \qquad (1)$$

where $\Delta\theta$ is the difference between the plasmon resonance angles with and without analytes, and the subscripts *NWSPR* and *SPR* represent a nanowire-enhanced SPR configuration and a conventional SPR scheme, respectively.

Figure 2 presents the calculated reflectance characteristics of a conventional and a nanowire-based SPR biosensor with the incidence angle. The SPR curves of a nanowire-based SPR configuration are for an inverse T-profile when GF = 0.75 and nanowire period Λ = 100 nm. Since SPR curves of a conventional SPR configuration with or without binding to analytes determined $\Delta\theta_{SPR}$ in Eq. (1) as 0.17º and the difference of resonance angles of the nanowire-based SPR biosensor with and without an analyte, $\Delta\theta_{NWSPR}$, was calculated to be 0.39º, using Eq. (1), the SEF is thus determined to be 2.29. Note that the reflectance amplitude and the width of SPR curves have also been affected by the presence of nanowires. While these parameters can be used to characterize the sensitivity enhancement as well, we focus on the behavior of the resonance angles since this provides the most convenient measure.

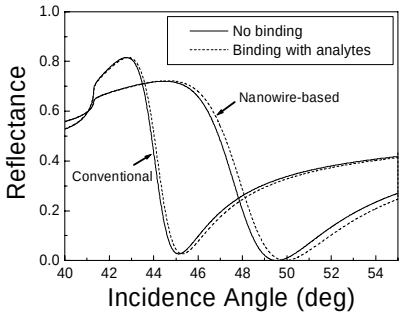

Fig. 2. SPR curves (reflectance vs. incidence angle) of SPR biosensors: for a conventional SPR biosensor, and for a nanowire-enhanced SPR biosensor of Fig. 1. Nanowires have an inverse T-profile at GF = 0.75, and nanowire period Λ = 100 nm. In both curves, no-binding on a bare gold film is represented with the solid line and binding with analytes with the dotted line.

Peak SEFs and the nanowire period Λ_{peak} at which the SEF is the highest are shown, respectively, in Fig. 3(a) and 3(b) for T- and inverse T-profiles, as the GF varies from 0 to 1. The numerical data of Fig. 3(a) show that a T-profile generally results in a higher SEF than an inverse T-profile. More specifically, the largest SEF achieved for a T-profile of nanowires is 47.35 at GF = 0.25, while the sensitivity enhancement for an inverse T-profile is 19.29 at the largest when GF = 0.9. The difference of the SEF with profiles is apparently caused by the varying strength of interactions between the substrate and nanowires, which may present different resonance properties. In order to investigate the sensitivity enhancement more thoroughly, the extinction spectra of a T-profile at GF = 0.25 which resulted in the highest SEF are displayed in the inset of Fig. 3(a). An extinction spectrum is frequently used to present optical properties of metallic nanostructures such as the resonant excitation of LSPs, and the position of extinction peaks corresponding to the region of the LSP resonant

#7078 - $15.00 US Received 6 April 2005; revised 27 April 2005; accepted 4 May 2005

excitation.[22,23] At GF = 0.25 and nanowire period Λ = 50 nm, the resonant wavelengths for T- and inverse T-profiles are, respectively, 647 nm and 716 nm as presented in the extinction spectra. Since a T-profile exhibits the extinction peak close to the incident wavelength λ = 633 nm, the extinction which correlates with the strength of LSPs is substantially improved at this wavelength. Such a large excitation of LSPs thus results in the highest sensitivity enhancement of 47.35 at GF = 0.25 and Λ = 50 nm as presented in Fig. 3(a).

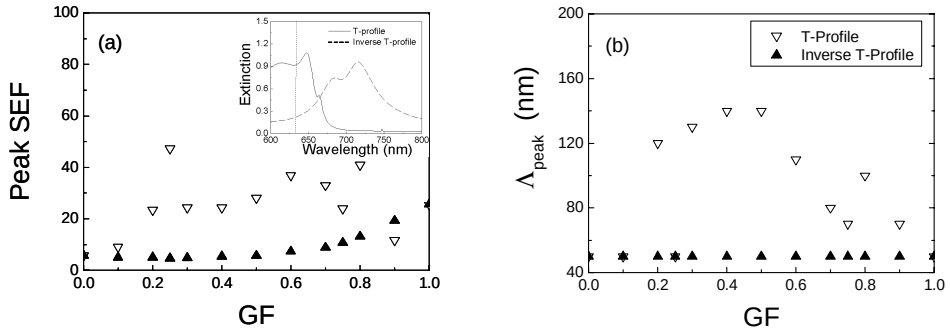

Fig. 3. (a) Peak SEF with GF for T-profile (▽) and inverse T-profile (▲). For each profile, GF is varied from 0 to 1. The inset shows extinction spectra for two different nanowire profiles with a T-profile in a solid line and an inverse T-profile in a dotted line. The vertical line in the extinction spectra indicates λ = 633 nm. For the inset, GF = 0.25 and nanowire period Λ = 50 nm. (b) Nanowire period Λ_{peak} when the SEF is the highest for each GF.

In short, two different mechanisms may be working for the sensitivity enhancement in a T- and inverse T-profile compared to the conventional SPR scheme. For a T-profile, LSP effect tends to be dominated since the excitation wavelength is near its extinction resonance and the resonance angle is far away from the SPP resonance angle. In the case of GF = 0.1 and 0.9, resonance angles of a T-profile are close to that of SPP modes, thus its LSP modes induce less sensitivity enhancement and the peak SEFs are comparable to or smaller than those of an inverse T-profile. For an inverse T-profile, SPP effect may still dominate and the presence of inverse T-profile nanowires changes the effective SPP feature of the gold film, possibly by non-resonant LSP. In particular, for a T-profile, the interactions of LSPs with SPPs are relatively small due to the limited interface between the gold film and nanowires, which leads to a giant amplification of the local electromagnetic field. Larger variation in SEF, higher sensitivity of the LSP to the environment change induced by analytes, and the LSP effects less interfered by interactions with a substrate are attributed to the better sensitivity of a T-profile structure. On the other hand, nanowires with an inverse T-profile have large interactions between LSPs and SPPs, and thus the excited LSP modes are damped and the enhancement of the sensitivity is minimal.

Figure 3(b) shows that nanowires of an inverse T-profile have the maximum sensitivity enhancement at Λ_{peak} = 50 nm regardless of the GF. However, for a T-profile, Λ_{peak} varies in the range of 50 nm to 140 nm. It is evident that an SPR biosensor with nanowires of a T-profile achieves a higher SEF at a larger period than an inverse T-profile. This implies that a T-profile offers a structure that is relatively easy to fabricate and can still provide excellent sensitivity enhancement. For this reason, further optimization is focused on nanowires with a T-profile. As an additional design parameter, the SEF width is defined as the range of the nanowire period, in which the SEF exceeds a given threshold value. While structural parameters in vertical dimension, such as the nanowire depth, can be constructed to nanometer accuracy, current fabrication techniques do not allow precise control of the nanowire period on a nanometer scale. Thus, achieving large SEF width as well as high SEF is crucial in the practical implementation of nanostructures based on such fabrication techniques. In other

#7078 - $15.00 US Received 6 April 2005; revised 27 April 2005; accepted 4 May 2005

words, if the SEF width can be designed to be sufficiently larger than the process deviation of a specific fabrication step, a nanowire-based SPR biosensor is minimally sensitive to fabrication errors as the reproducibility and reliability of the sensor performance can be enhanced. In this study, the threshold of SEF is fixed at 20, which is approximately the maximum SEF obtained with an inverse T-profile. Thus, zero SEF width means that the peak SEF is always lower than the threshold with any nanowire period. The maximum SEF width was obtained at GF = 0.5, as shown in Fig. 4(a), and determined to be 66.3 nm. The SEF characteristics in Fig. 4(b) show fairly broad and robust performance with the nanowire period. Note that the SEF drops abruptly at 95 nm and 187 nm due to a destructive coupling mechanism between nanowires when LSPs are driven out of phase and result in destructive interactions with different magnitudes of SEF reduction.[24] The resonance angles at GF = 0.5 and Λ = 140 nm with and without an analyte are respectively 49.14º and 53.93º, and thus SEF of Eq. (1) is calculated to be 28.17. While LSP modes excited in nanowires are created at lower momentum, the negative shift of resonance angle observed in this optimum geometry does not adversely affect the sensing of an SPR biosensor as long as the nature of the shift is *a priori* known.

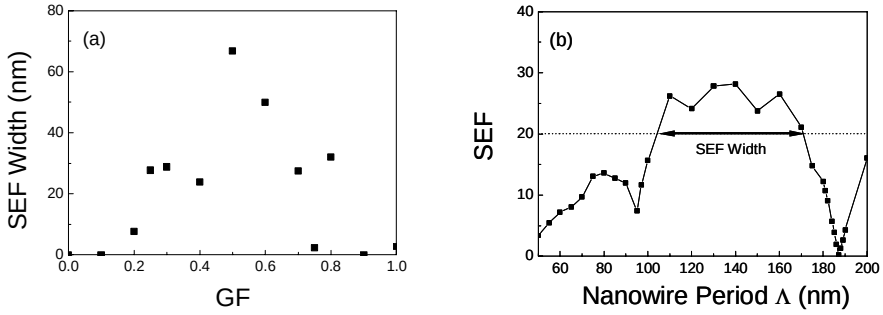

Fig. 4. (a) The SEF width defined as the range of nanowire periods in which the SEF exceed a given SEF threshold in the SEF characteristics, as GF varies from 0 to 1. The threshold used to determine the SET width is 20. (b) Plot of SEF characteristics of a T-profile at GF = 0.5.

4. Concluding remarks

We have investigated the sensitivity enhancement of nanowire-based SPR biosensors using the RCWA method. We have confirmed that the use of nanowires enhances the sensitivity significantly. It was found that nanowires of a T-profile in general show a higher SEF than those of an inverse T-profile. The maximum SEF achieved was 47.35 with nanowires of a T-profile and GF = 0.25. In view of the sensitivity performance and the reliability of an implementation, an optimal nanowire geometry is a T-profile (w_{top} is 40 nm and w_{bottom} is 20 nm) with GF = 0.5 (d_{top} and d_{bottom} are equal to 10 nm). The optimized structure can achieve the peak SEF as high as 28.17 at Λ_{peak} = 140 nm. The SEF width calculated with the threshold SEF at 20 is 66.3 nm. This is sufficiently large enough to minimize the performance deviation due to fabrication errors. Our study on a nanowire-enhanced SPR biosensor demonstrates the potential for significant improvement of the sensitivity of an optimal nanowire structure and experimental work is currently under way.

Acknowledgments

The authors acknowledge the support by the Nano-Bioelectronics and Systems Research Center of Seoul National University, which is an ERC sponsored by the Korean Science and Engineering Foundation.